J. Membrane Biol. 108, 153–164 (1989)

The Journal of
Membrane Biology

Ion Permeation in a K^+ Channel in *Chara australis:* Direct Evidence for Diffusion Limitation of Ion Flow in a Maxi-K Channel

D.R. Laver, K.A. Fairley, and N.A. Walker
Biophysics Laboratory, School of Biological Sciences, The University of Sydney A12, New South Wales 2006, Australia

Summary. We report a study of a potassium-selective channel in the membrane delineating cytoplasmic drops from *Chara australis*. The relatively large conductance (170 pS in 150 mol/m^3 (mM) KCl), high ion selectivity ($P_{Cl}/P_K = 0.015 \pm 0.01$) and voltage-dependent kinetics of this channel indicate that it is a type of maxi-K channel commonly found in animal cells but not previously detected in any plant cell.

The current-voltage (I/V) characteristic of these channels was examined in drop-attached and in excised outside-out patches using the patch-clamp technique, over the unusually large voltage range of −250 to 200 mV. The I/V characteristic is nonlinear and shows saturation at extreme voltages; the current also saturates at high [K^+]. In solutions with symmetrical KCl concentrations the saturation behavior of the current is asymmetrical. The permeability of the channel depends on whether it is observed in excised or in drop-attached membrane patches.

Here we investigate the main factors affecting the permeation of K^+ ions through this maxi-K channel. We present the first direct evidence for the importance of diffusion external to the pore in limiting ion flow through maxi-K channels. The data are consistent with an ion translocation mechanism whose current is limited (i) at high voltages by ion diffusion external to the pore and (ii) at high [K^+] by the maximum transport rate of the channel. We fit the data to a diffusion-limited pore model in which the pore exhibits saturation described by Michaelis-Menten kinetics with a $K_m = 50 \pm 25$ mol/m^3 and $G_{max} = 300 \pm 20$ pS.

Key Words K^+ channel · permeation kinetics · patch clamp · *Chara australis* · cytoplasmic drop · diffusion limited

Introduction

One of the first channel types studied by the patch-clamp technique was a high conductance potassium-selective channel, which has since been referred to as BK (Marty, 1983; Blatz & Magleby, 1987) or as maxi-K (Latorre & Miller, 1983). Maxi-K channels show potential-dependent kinetics and exist in both calcium-activated and noncalcium-activated forms. They are believed to play a role in membrane excitability and in excretion (Latorre & Miller, 1983; Blatz & Magleby, 1987). Maxi-K channels are ubiquitous among animal cell types but have not been identified in any plant cells other than those of *Charophytes*.

Here we report on the potassium-selective channel found in the membrane delineating cytoplasmic drops from *Chara australis*. The large unit conductance (170 pS at [KCl] = 150 mol/m^3), high selectivity for K^+ over other cations and the voltage-dependent nature of the ion-gating kinetics of this channel (Lühring, 1986; Laver & Walker, 1987) indicate that it is of the maxi-K type.

Fluorescent labeling of the tonoplast (Lühring, 1986; Sakano & Tazawa, 1986) suggests that the membrane around the cytoplasmic drop is derived wholly or in part from the tonoplast of the parent cell. Potassium ions are normally at equilibrium across this membrane. Interestingly, the time-averaged voltage-dependent behavior of this channel permeability is similar to that found for the potassium permeability of the *Chara* plasmalemma (Laver & Walker, 1987). The role of the maxi-K channel in *C. australis* is not yet understood.

We report here measurements of the unitary currents through the maxi-K channel in both excised and attached membrane patches of cytoplasmic drops from *C. australis* using the patch-clamp technique.

In principle, the current through a channel depends on both the conductance of the pore and that of the aqueous medium near the pore entrance. If the latter conductance is low enough the diffusion of ions to the pore mouth will limit the current through the pore. The ion concentrations and electric potentials within approximately 1 nm of the pore mouths will differ from those in the bulk phases, and the current will saturate at high voltages. The extent of the diffusion limitation depends not only on the relative conductances of the pore interior and mouths but also on the nature of the

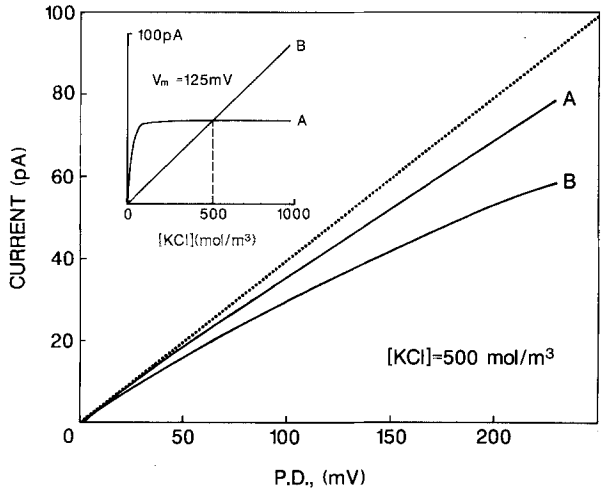

Fig. 1. The diffusion-limited I/V characteristics of two hypothetical pores: (*A*) a saturating pore; (*B*) a pore with linear concentration dependence. The solid I/V curves were calculated from Eqs. (A1)–(A3) using $n = 9$ (*see* Discussion) and $P'_c = P''_c = 2 \times 10^{-18}$ m³/sec. The dotted line shows the intrinsic I/V characteristics of both pores (i.e., $P_c = \infty$), and the insert shows their concentration dependences. It is clear that the pore with the nonsaturating concentration dependence ($K_m = 10^4$ mol/m³) (*B*) is more limited for a given value of P_c than the saturated pore ($K_m = 0.1$ mol/m³) (*A*)

concentration dependence of the current. This is illustrated in Fig. 1 where the I/V characteristic is more linear, less limited, for a saturated pore than for one far from saturation. This is because in a saturated pore the current is less dependent on ion concentration at the pore mouths.

Neglecting diffusion limitation that may exist will lead to erroneous conclusions concerning ion-channel interactions (Andersen, 1983). Therefore the crucial issue for a study of permeation mechanisms is whether ion diffusion in the aqueous phases measurably limits the current. The voltage-dependent Na^+ blockade of Ca^{2+}-activated K^+ channels in chromaffin cells (Yellen, 1984) suggests that diffusion-limited ion flow is important for this channel. It is known that ion permeation through gramicidin channels is limited by ion diffusion external to the pore (Anderson & Procopio, 1980; Andersen, 1983).

Here we estimate the magnitude of the effects of ion diffusion near the pore mouth part of the protocol used by Andersen (1983). We will examine the factors affecting ion permeation through the *Chara* maxi-K channel and show that it is diffusion limited.

Materials and Methods

Cytoplasmic drops were formed from the internodal cells of *Chara australis* R. Brown and from another, corticated, *Chara* species,[1] using the method of Kamiya and Kuroda (1957). Single-channel currents were observed in both drop-attached and excised outside-out membrane patches. Methods for achieving these membrane patch configurations are described by Hamill et al. (1981). Exchange of bathing media was achieved using the "sleeve" technique of Quartararo and Barry (1987) whereby the excised patch is transferred between baths containing different solutions. During experiments on drop-attached patches the composition of the medium bathing the cytoplasmic drops was 150 mol/m³ KCl, 5 mol/m³ $CaCl_2$, 5 mol/m³ H^+MES, adjusted to pH 5.2 (the vacuolar pH) using KOH. The pipette filling solutions for drop-attached patches and the bathing medium for the outside face of excised outside-out patches were the same. These contained KCl at concentrations ranging from 10 mol/m³ to 1000 mol/m³ and adjusted to pH 5.2. The concentrations of $CaCl_2$ and H^+MES were approximately 3% of that of KCl up to a maximum of 5 mol/m³. The pipette filling solutions for excised outside-out patches contained KCl, 1–2 mol/m³ EGTA and 5 mol/m³ H^+MES; they were adjusted to pH 7.1 with KOH, and to pCa 7 to 9 with $CaCl_2$. The channel conductance was unaffected by the calcium concentration over this range. Experiments were performed at 23 ± 2°C.

Glass micropipettes were made with a vertical electrode puller (David Kopf model 720) using a two-stage pulling process. Micropipettes used for drop-attached patches were made from both soda glass (Drumond Scientific) and from borosilicate glass (Vitrex BRI/E), whereas those used for excised patches were made from borosilicate glass and were fire-polished before use. Silgard® coating was not necessary for good patch records and was omitted.

The details of the experimental protocol and the recording and display apparatus have been described previously by Laver and Walker (1987). Briefly, upon achieving a high resistance seal (10–50 GΩ) between the membrane patch and the micropipette, the pipette potential was clamped to a random sequence of values over the range ±250 mV at 10-sec intervals. The time course of the transmembrane current and pipette potential were recorded simultaneously on magnetic tape using FM encoding. The current and voltage recordings were later digitized and redisplayed using a CRO for graphics display. Unitary currents were measured from the size of the current steps. The calibration of the recording system was made at the beginning and end of each tape cassette by recording a square waveform with 5 V amplitude. The estimated error on the current measurements is ±0.3 pA or ±2% over the voltage range ±200 mV. The error in the current measurements at membrane potentials more negative than −200 mV is ± 1 pA due to the relatively short open times of the channel at these potentials.

[1] At the time of these experiments we were unaware that one culture of *Chara australis* also contained small amounts of a corticated species of *Chara*. Cytoplasmic drops formed from the corticated species also contain a maxi-K channel with apparently identical permeation and gating characteristics to those in *C. australis*. It is possible that some of the results shown in this study are derived from maxi-K channels from this other species of *Chara*.

The potential difference across the membrane patch (V_m) was calculated from the pipette command potential (V_c) at the patch-clamp amplifier. In the case of excised outside-out patches

$$V_m = V_c - (V_e - V_L) \quad (1)$$

and in the case of drop-attached membrane patches

$$V_m = -V_c + V_r + (V_e - V_L) \quad (2)$$

where V_L, V_r and V_e are the liquid-junction potential, the resting potential of the membrane outside the patch, and the zero-current electrode potential, respectively (all with respect to the bath electrode). The resting potential was measured at the end of each run of measurements on a drop-attached patch by breaking the membrane patch using suction and measuring the pipette potential required to achieve zero current. Values of V_r were typically in the range ±20 mV. The pipette and earth electrodes were silver-chloride-coated silver wire. The zero-current potential difference between the electrodes was measured before sealing the pipette against the drop membrane, and again at the termination of each membrane patch. The liquid-junction potential is calculated using the Henderson equation (Barry & Diamond, 1970).

Theoretical predictions shown here are solutions to the three simultaneous equations (A1)–(A3) (*see* Appendix). These equations were solved numerically for the parameters, y', y'' and J, using the false-position method, on a Compaq-386 mini computer. Theoretical nonlinear fitting of the data was done using the least-squares criterion, found by the method of steepest descent. Error estimates for the fit parameters represent 90% confidence limits, which were calculated from linear approximations to Eqs. (A1)–(A3).

Results

General Observations

High resistance seals (10–50 GΩ) formed readily and were stable. Seals with drop-attached patches are markedly less stable at positive membrane potentials (i.e., negative pipette potentials) than at negative membrane potentials. Furthermore, seal breakdown at negative pipette potentials could often be reversed by the application of positive potentials. However, this is not so with excised patches, which are stable over the voltage range ±200 mV. Seals against drop-attached patches could withstand larger negative membrane potentials (−250 to −300 mV) than seals with excised patches. The background current noise of the membrane patch and micropipettes is 1 pA root mean square (rms) for borosilicate glass and 2 pA rms (5 kHz bandwidth) for soda glass pipettes.

The ion gating kinetics of this channel are known to be voltage dependent (Lühring, 1986; Laver & Walker, 1987). Open state durations are very short at extreme negative membrane potentials so that the apparently current amplitude is reduced by the limited bandwidth of the recording system. At positive membrane potentials the probability of channel opening is small, so there are relatively few data at these potentials. Thus measurements of the I/V characteristics are mainly restricted to the voltage range −250 to +50 mV for drop-attached patches and ±200 mV for excised outside-out patches. Two types of K^+ channels with large conductances (170 and 130 pS) have been detected in cytoplasmic drops. The channel studied here has the larger conductance and is more frequently detected in membrane patches. In this work the channel is identified in patch recordings by its I/V characteristic.

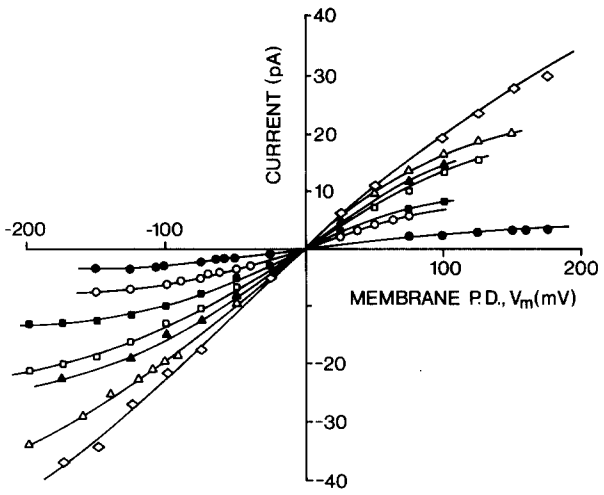

Fig. 2. The I/V characteristics of the maxi-K channel in excised outside-out patches in symmetric KCl solutions. The magnitude of the unitary currents increased with increasing [KCl]. The KCl concentrations are (mol/m³): ●—10(6); ○—25(4); ■—50(3); □—100(5); ▲—200(1); △—300(3); ◇—500(2). The number in parentheses indicates the number of membrane patches recorded. The solid curves are polynomial fits of order 3–5 to the data

Single-Channel Current: Voltage and [KCl] Dependence

Variation between the I/V characteristics obtained from different patches, in the same media, is less than ±1 pA. Those measured in excised patches in the presence of symmetrical KCl concentrations are shown in Figs. 2 and 3. The current shows saturation at extreme membrane potentials, and this saturation is not symmetrical with membrane potential. The nonlinearity is most evident over the concentration range 25–200 mol/m³. The seven values of

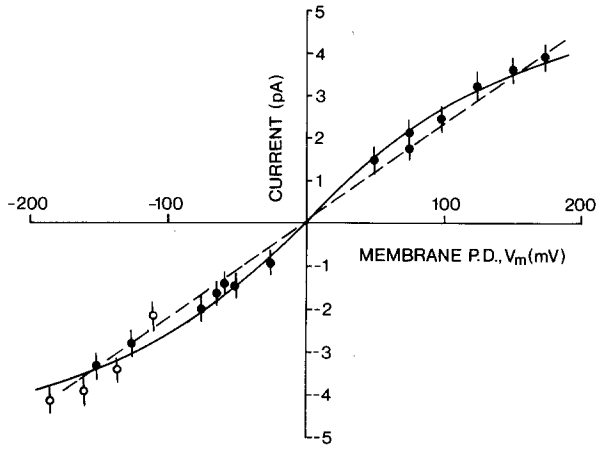

Fig. 3. The *I/V* characteristics of the maxi-K channel at low KCl concentrations. (●)—$[KCl]_i = [KCl]_o$ = 10 mol/m³; (○)—$[KCl]_o$ = 10 mol/m³, $[KCl]_i$ = 100 mol/m³. The error bars indicate the measurement accuracy. The dashed line is a linear fit to the full circles. The solid curve is the predicted *I/V* characteristics for a diffusion-limited pore with K_m = 40 mol/m³, G_m = 300 pS, P_c = 3.5 × 10^{-18} m³/sec

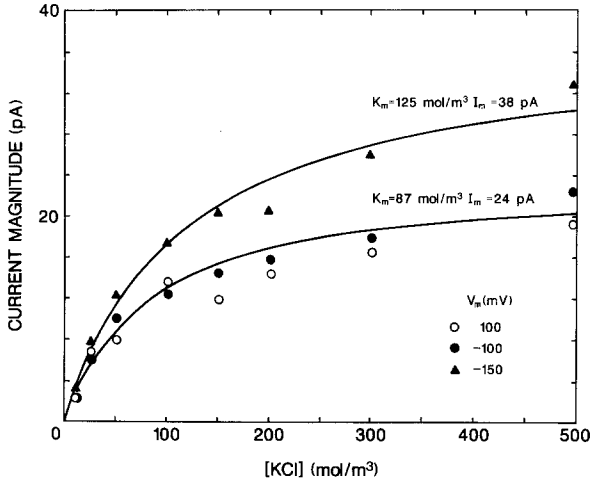

Fig. 4. The concentration dependence of the maxi-K channel current in excised outside-out patches at three membrane potentials. The data is derived from the polynomial fits to the data in Fig. 2. The asymmetry of the *I/V* characteristic of the channel is seen here as a difference between the current at 100 and at −100 mV. The solid curves are least-squares fits of the Michaelis-Menten equation to the data

the reversal potential, derived from polynomial fits to the data in Fig. 2, lie between 3 and −3 mV over the concentration range 10 mol/m³ to 500 mol/m³. The concentration-dependence of the single-channel current, shown in Fig. 4, is derived from the polynomial fits to the data in Fig. 2. This data has also been corrected for small differences in the ambient temperature between experiments by assuming a thermal Q_{10} of 1.4 for the channel conductance.[2] These corrections were all less than 5%. The current shows a hyperbolic dependence on KCl concentration with a half-maximum at 100 mol/m³.

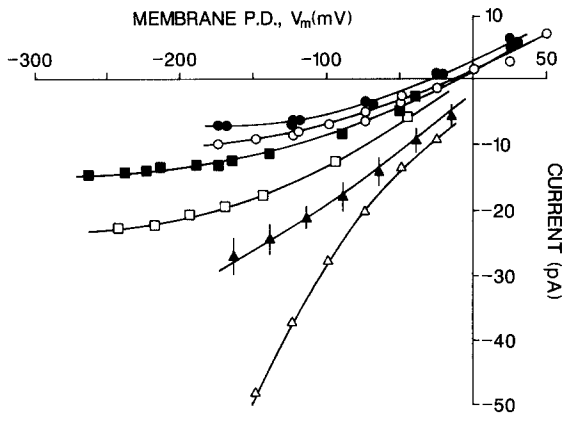

Fig. 5. The *I/V* characteristics of drop-attached patches. The number of membrane patches recorded at each concentration are (symbol—[KCl] mol/m³ (#)): ●—12(3); ○—25(2); ■—50(5); □—100(1); ▲—200(3); △—1000(2). The solid curves are polynomial fits of the data. The error bars indicate the variation in the results from three patches

Figure 5 shows the *I/V* characteristic obtained in drop-attached patches over the concentration range 12 to 1000 mol/m³. The reversal potentials indicate [K^+] of 50 to 100 mol/m³ inside the cytoplasmic drop over the external concentration range 12 to 150 mol/m³. The currents in excised and drop-attached patches are compared in Fig. 6. With potassium concentrations of less than 50 mol/m³ in the patch pipette, the currents differed significantly between the drop-attached and excised patches. Equalizing the osmotic potential of each side of drop-attached patches using sorbitol (at 260 mol/m³ in the pipette) had no effect on the currents when [KCl] was 12 mol/m³. Figure 7 shows the channel *I/V* characteristics in excised patches in asymmetric concentrations of KCl. The reversal potential, V_R, for the channel separating solutions containing 3.5 mol/m³ (inside) and 150 mol/m³ (outside), determined from the *I/V* data using polynomial interpolation, is 83 ± 10 mV. The relative permeability for chloride ions in the channel (P_{Cl}/P_K), calculated from V_R using the Generalized Null Potential equation (Barry & Gage, 1984), was found to be 0.015 ± 0.01.

[2] A thermal Q_{10} of 1.4 has been measured for the maxi-K channel from rat muscle (Barrett, Magleby & Pallotta, 1982). As the thermal corrections to the data are small, it will suffice to use this value for the present work.

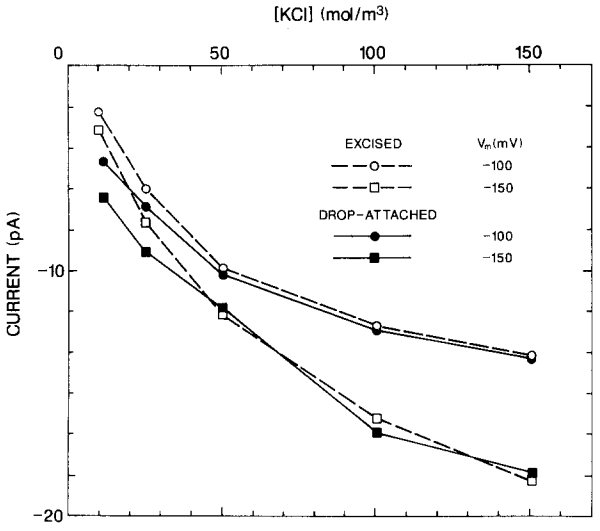

Fig. 6. The comparison of unitary currents in excised outside-out and drop-attached patches at two membrane potentials. For drop-attached patches [KCl] refers to the concentration in the patch pipette, whereas for excised patches the concentrations are equal on each side of the membrane. When [KCl] is less than 50 mol/m³ the channel current in drop-attached patches is significantly larger than in excised patches

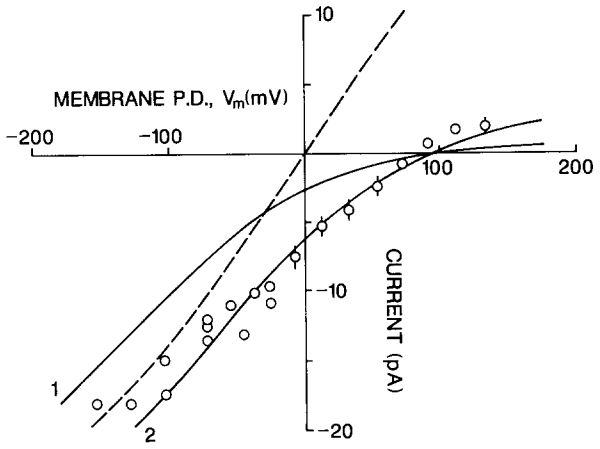

Fig. 7. The *I/V* characteristics of the maxi-K channel in an excised outside-out patch. (○) $[KCl]_i$ = 3.5 mol/m³, $[KCl]_o$ = 150 mol/m³ (several channels in one patch). The solid curves are the predictions of Eqs. (A1)–(A3) for asymmetric KCl solutions (3.5 and 150 mol/m³) with K_m = 20 mol/m³, G_{max} = 300 pS and P_c'' = 1.1×10^{-18} m³/sec; (*1*) P_c' = 1.1×10^{-18} m³/sec and (*2*) P_c' = 1.1×10^{-17} m³/sec. Good fits to the data were obtained for values of P_c' = $(1.1 \pm 0.3) \times 10^{-17}$ m³/sec. Comparison of solid curves (*1* and *2*) show the predicted effect of the addition of an impermeant cation (curve *2*) (20–30 mol/m³) to the inside solution. The deviation of curve *2* from the data at positive membrane potentials is due to the finite chloride permeability of the channel which has been neglected in the theory. The dashed curve shows a least-squares fit to the data from channels in symmetric solutions containing 150 mol/m³ KCl where P_c'' = 1.1×10^{-18} m³/sec and P_c' = P_c''

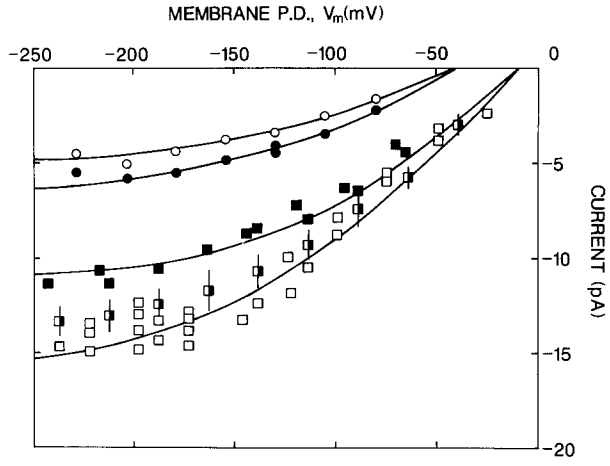

Fig. 8. The effects of urea and sucrose in the pipette solutions on the *I/V* characteristics of the maxi-K channel in drop-attached membrane patches. The pipette solutions are (symbol — composition (number of patches recorded)): □—50 mol/m³ (3); ■—[KCl] = 50 mol/m³, [sucrose] = 700 mol/m³ (2); ◨—[KCl] = 50 mol/m³, [urea] = 700–750 mol/m³ (3); ●—[KCl] = 10 mol/m³, [urea] = 750 mol/m³ (1); ○—[KCl] = 10 mol/m³, [sucrose] = 580 mol/m³ (1). The error bars indicate the variation in the results from three patches. The solid curves show the predictions of the diffusion-limited pore model and the effect of a 30% decrease in the aqueous convergence permeation constants, P_c, i.e., from 1.8×10^{-18} to 1.26×10^{-18} m³/sec for [KCl] = 50 mol/m³ and from 3.8×10^{-18} to 2.6×10^{-18} m³/sec for [KCl] = 10 mol/m³

I/V Curves: Effect of Sucrose and Urea

The effects of sucrose (700 mol/m³) and urea (750 mol/m³) in the patch pipette on the currents in drop-attached patches are shown in Fig. 8. Figure 9 shows the effect of the addition and removal of sucrose (700 mol/m³) to the bathing medium on the *I/V* characteristics of an excised outside-out patch. The effect of sucrose is significant and completely reversible. The effects of isosmotic concentrations of sucrose (580 mol/m³) and urea (750 mol/m³) are compared in Fig. 10. Addition of sucrose to the medium with excised and drop-attached patches significantly decreases the current. Urea had less than half the effect of sucrose.

Discussion

Is Current through the Maxi-K Channel Diffusion-Limited?

Andersen (1983) demonstrated the importance of diffusion-limitation effects to ion permeation in gramicidin by measuring the effect on the current of independently manipulating the ion permeabilities

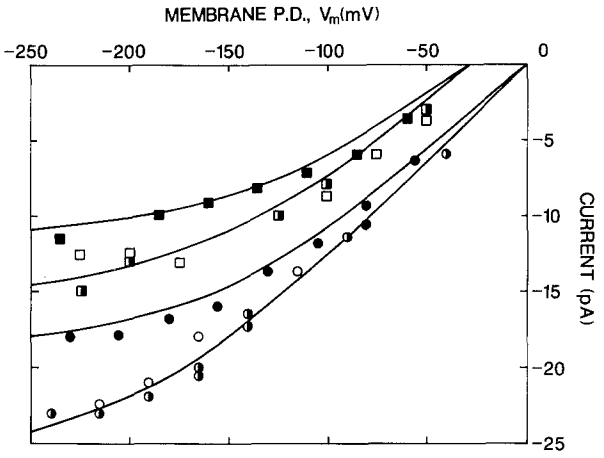

Fig. 9. The effect of sucrose in the bulk aqueous phases on the *I/V* characteristics of a maxi-K channel in an excised outside-out patch at two KCl concentrations. The pipette solution contained KCl (150 mol/m^3) and sucrose (700 mol/m^3). In chronological order the external bathing media are: ○—[KCl] = 150 mol/m^3; ●—sucrose (700 mol/m^3) added to bath; ◑—sucrose removed; □—[KCl] = 50 mol/m^3; ■—sucrose (700 mol/m^3) added to bath; ◨—sucrose removed. The solid curves show the predictions of the diffusion-limited pore model and the effect of a 35% decrease in the aqueous convergence permeation constants, P_c, i.e., from 1.8×10^{-18} to 1.26×10^{-18} m^3/sec for [KCl] = 50 mol/m^3 and from 1.0×10^{-18} to 0.7×10^{-18} m^3/sec for [KCl] = 150 mol/m^3

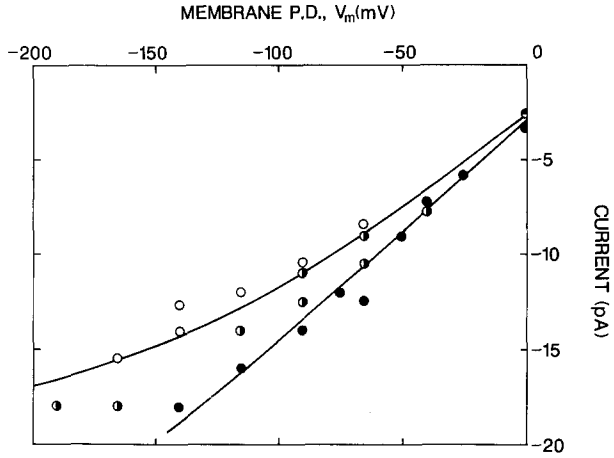

Fig. 10. The comparative effects of urea and sucrose in the bulk aqueous phases on the *I/V* characteristics of two maxi-K channels. The pipette solution contained KCl (50 mol/m^3) and urea (750 mol/m^3). The external bathing media are; ●—[KCl] = 150 mol/m^3; ○—[KCl] = 150 mol/m^3 + sucrose (580 mol/m^3); ◑—[KCl] = 150 mol/m^3 + urea (750 mol/m^3). The solid curves show the predictions of the diffusion-limited pore model and the effect of a 35% decrease in the aqueous convergence permeation constants, P_c, i.e., from 1.0×10^{-18} to 0.65×10^{-18} m^3/sec

inside and outside the channel. Here, part of his protocol is used to test for the importance of diffusion-limitation; the effects of sucrose and urea on the *I/V* curves are measured. The rationale for this test is given in detail by Andersen (1983). Briefly, the addition of 20% (580 mol/m^3) sucrose to the aqueous phases reduces the diffusion coefficient of potassium ions by 35% (*see* Table II in Andersen, 1983) and so is expected to decrease the permeance of the aqueous convergence regions by up to 35%. It is unlikely that a molecule as large as sucrose (Stokes radius about 0.47 nm) will alter the intrinsic properties of the channel by penetrating the pore interior.

The addition of sucrose to the solutions will decrease the water potential and affect the ion activity coefficients. The effect of water potential on the conductivity of the maxi-K channel is not known. The conductivity of gramicidin channels may be dependent on the water potential (Andersen, 1983) but that of the voltage-dependent anion channel from mitochondria is not (Zimmerberg & Parsegian, 1986). To investigate the effect of changes in water potential on the channel current, the effect of urea (750 mol/m^3) on the channel current was measured. Urea at 750 mol/m^3 has the same effect on the water potential as sucrose (580 mol/m^3). However, urea and sucrose have markedly different effects on the ion mobility. Urea at 750 mol/m^3 reduces the diffusion coefficient of potassium ions by only 5%.

In these experiments we estimate that the mean activity coefficient[3] of KCl is reduced by 3% by urea (Kundu & Das, 1979). The effects of sucrose (250 mol/m^3) (Harned & Shropshire, 1958) on the mean activity of KCl and sucrose (1000 mol/m^3) on that of NaCl (Robinson, Stokes & Marsh, 1970) suggest that it has less than 3% effect on the activity of K^+ in the bulk phases.

The results in Figs. 8–10 demonstrate an effect similar to that observed in gramicidin channels (Andersen, 1983). Sucrose at concentrations ranging from 580–700 mol/m^3 caused a marked reduction in the unitary current, whereas the addition of urea (750 mol/m^3) has a smaller effect. The sucrose effect was too large to be due to changes in ion activity alone. The effect of adding and removing sucrose from the aqueous phase surrounding individual membrane patches was investigated (*see* Figs. 9 and

[3] Strictly speaking, the single-ion activity coefficients for K^+ should be used. However, absolute values of single-ion activities are not attainable. The general consensus is to consider that the single-ion activities for K^+ and Cl^- are equal to their mean value.

Table 1. The summary of the results of the analysis of the data shown in Figs. 8 and 9 in terms of the diffusion-limited pore model[a]

		$[KCl]_o$ (mol/m^3)	$[KCl]_i$ (mol/m^3)	P_c (10^{-18} m^3/sec)	G_{max} pS	P_c^a (10^{-18} m^3/sec)
Cell-attached patch	Bare	50	100	2.0 ± 0.25	335 ± 140	2.10 ± 0.07
	Sucrose	50	100	1.45 ± 0.11	286 ± 70	1.42 ± 0.04
	Urea	50	100	1.6 ± 0.07	460 ± 85	1.82 ± 0.04
Excised patch	Bare	150	150	1.07 ± 0.08	275 ± 4	1.02 ± 0.02
	Sucrose	150	150	0.73 ± 0.04	390 ± 8	0.78 ± 0.02
	Bare	50	150	1.66 ± 0.16	540 ± 150	1.97 ± 0.1
	Sucrose	50	150	1.38 ± 0.09	369 ± 8	1.47 ± 0.04

[a] The parameter K_m is set to 25 mol/m^3. The fitted variables are P_c and G_{max}. G_{max}, for a given [KCl] is proportional to the intrinsic permeance of the pore. The errors shown are 90% confidence limits. P_c^a are fitted values of P_c where G_{max} is held constant at 310 pS.

10) to ensure that supposed changes in channel conductance were not artifacts of observing different channel populations. In some cases the large differences in water potential on each side of the patch could result in significant transmembrane water flows. *I/V* curves from channels in symmetric 150 mol/m^3 KCl with (Fig. 9) and without (Figs. 4, 6 and 12) high internal urea concentrations, indicates that osmotic water flow has no significant effect on the current in these experiments.

The effects of sucrose and urea (*see* Figs. 8 and 9) were fitted with Eqs. (A1)–(A3) (fits not shown) where fit parameters were P_c and G_{max} (for a given [KCl] G_{max} is proportional to the intrinsic permeance of the pore). The results of this analysis are summarized in Table 1. Sucrose significantly reduced P_c but had neither a consistent nor significant effect on G_{max}. So it appears that sucrose acts by reducing the permeance of the aqueous regions rather than that of the pore itself. Hence changes in water potential upon the addition of sucrose do not significantly affect the channel permeance. The data was also fitted for the case when G_{max} is held constant (*see* Table 1). Here sucrose was found to decrease P_c by 25–30%.

The effect of urea on the *I/V* characteristic is difficult to interpret. Curiously, urea had a larger effect than expected from its effect on ionic mobilities alone, which is possibly due to a reduction in the activity of K^+ in the bulk phases. Alternatively, the data in Table 1 suggest that urea may act by altering permeabilities of the convergence regions, though this is by no means certain.

The greater effect of sucrose than of urea indicates that the maxi-K channel, like the gramicidin channel, is diffusion limited. This hypothesis is also supported by the data in Table 1. This provides the first direct evidence for the importance of diffusion limitation of ion flow through maxi-K channels.

A more exact analysis of the effect of sucrose is not possible because the concentration of sucrose near the membrane may be less than that in the bulk phases (Andersen, 1983). However, an upper limit to the permeation constant, P_c, can be found by assuming that the sucrose concentration near the pore mouths is equal to that in the bulk phases, that P_c decreases by 35% upon the addition of sucrose and by fitting the observed decrease in channel conductance with Eqs. (A1)–(A3). If the pore is saturated (in the extreme case when K_m = 1 mol/m^3), with $[K^+]$ in the range 50–150 mol/m^3, P_c must be less than 2.10^{-18} m^3/sec in order to account for the magnitude of the effect of sucrose. When the pore is assumed to be far from saturation (K_m = 10^4 mol/m^3) P_c must be less than 5.10^{-18} m^3/sec.

Diffusion-Limited Currents across Patches in Asymmetric Solutions

One way to gauge the importance of diffusion-limitation effects at very low ion concentrations is to measure the channel *I/V* characteristics in asymmetric solutions.

Close scrutiny of the theoretical curves (*1* and *2*) in Fig. 7 reveals an effect peculiar to diffusion-limited ion flow. In this case the current flowing into the pipette (i.e., flowing from high $[KCl]_o$ (150 mol/m^3 outside) to low $[KCl]_i$ (3.5 mol/m^3 inside)) is limited mainly by ion diffusion in the aqueous convergence regions at the inside pore mouth. An increase in the ionic strength or moderate increase in $[K^+]$ of the inside solution increases the inward K^+ current (at fixed V_m). This is because it is possible for a large fraction of the potential difference between the bulk phases to occur across the aqueous region at the inside pore mouth. Increasing the ionic strength of the inside medium acts to screen the

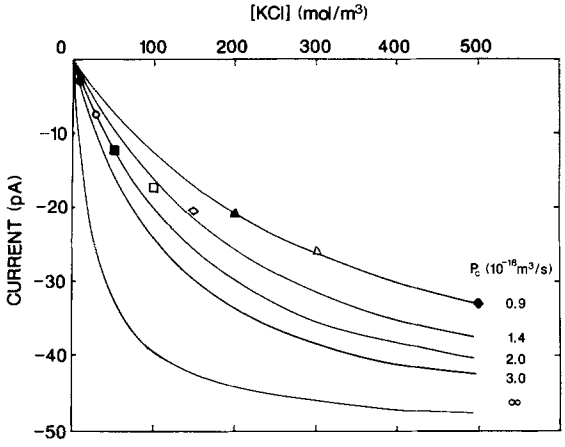

Fig. 11. The concentration dependence of single-channel currents from Fig. 4 ($V_m = -150$ mV) is compared to solutions of the simultaneous equations (A1)–(A3) for several values of the permeation constants, P_c, of the aqueous convergence regions. The pore has $K_m = 30$ mol/m³ and $G_{max} = 310$ pS. The predicted intrinsic [KCl] dependence of the pore is that for which $P_c = \infty$

electric field near the pore mouth; increasing the fraction of the potential difference across the pore, thus increasing the driving force on the permeant ions within the pore. Further, at low $[KCl]_i$, K^+ ions inside the pipette contribute little to the net ion flow through the channel. Hence increasing $[KCl]_i$ can enhance the inward K^+ current as shown in Fig. 7.

What does this mean to the electrophysiologist? A common tool used for determining the ion species permeable in a particular channel population is examining the effect of changes in the ionic composition of the cell-bathing medium on the permeation characteristics of the plasma membrane. However, the plasma membranes of plant cells are often bathed in media of low ionic strength (less than 1 mol/m³). If a particular population of channels is diffusion-limited then an increase in the ionic strength of the bathing medium of the cell will enhance the outward flow of permeable ions from the cell. Effects like this have been observed in voltage-clamp studies of *C. australis* (M. Beilby, *personal communication*).

It is possible to deduce a lower limit to the parameter P_c at low [KCl] from the attenuating effect of a reduction in $[KCl]_i$ (from 150 to 3.5 mol/m³) on the inward current and comparing this to solutions of Eqs. (A1)–(A3) (*see* Fig. 7). The lower bound on P_c, like the upper (*see* previous section), depends on whether or not the pore is near saturation. The minimum value of P_c, with [KCl] = 3.5 mol/m³, in a saturated pore is 4.0×10^{-18} m³/sec, whereas for a pore far from saturation and lower bound for P_c is 2.0×10^{-17} m³/sec. The insensitivity of the current (for V_m more negative than -100 mV) to $[KCl]_i$ (*compare* the data in Fig. 7 with the dashed line) indicates that ion diffusion at the pore mouth does not significantly limit the current at these low ion concentrations.

Regardless of the assumed degree of pore saturation the lower limit of P_c deduced from the data at low ion concentrations (above) is 2–3 times larger than the upper limit for P_c at [KCl] = 150 mol/m³ determined from the sucrose experiments: hence P_c must be concentration-dependent. This does not necessarily indicate a concentration dependence in the ion diffusion coefficients but rather reflects the inability of the neutral, right circular cylinder to model real channels. Figure 11 compares the K^+ concentration dependence of current with solution of Eqs. (A1)–(A3) for several values of P_c.

Modelling the *I/V* and [KCl] Dependences

So far, we have concluded that the channel is diffusion limited and that P_c is concentration dependent. We have done this without making assertions about the intrinsic properties of the pore. An attempt is made here to model the *I/V* and [KCl] dependences in terms of a diffusion-limited pore in order to unravel the kinetics of ion permeation within the pore from diffusion-limitation effects and to provide a basis on which the effects of channel modifiers can be studied.

It has proved difficult to interpret quantitatively the permeation characteristics of the channel in terms of the theory of diffusion limitation. The difficulty, in part, is that it is hard to discern which characteristics of ion permeation are attributable to intrinsic properties of the channel and which arise from diffusion-limitation effects (e.g. the curvature of the *I/V* characteristic). These problems are compounded by the fact that there are no satisfactory models for diffusion-limited ion flow through charged pores with unknown geometry. Hence the relationship between P_c and the geometric parameters of the pore are more tenuous than that implied by Eq. (A4).

Therefore the diffusion-limited pore model used here contains several assumptions. First, Michaelis-Menten kinetics were chosen as the simplest way of representing the saturation of current at high K^+ concentrations.

Second, ion diffusion in the pore is assumed to be consistent with electrodiffusion theory, i.e., the permeance of the pore is independent of voltage.

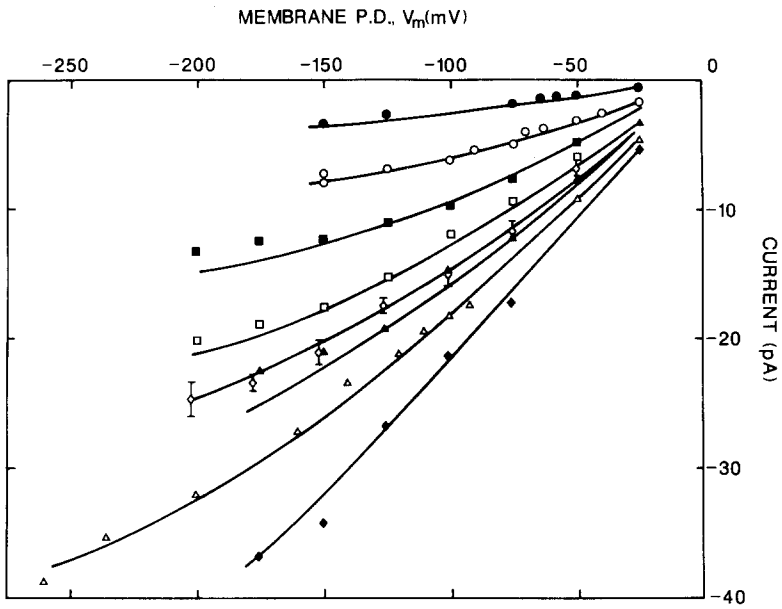

Fig. 12. The *I/V* characteristics of the maxi-K channel in excised patches including some data from Fig. 2. The KCl concentrations associated with each datum symbol are the same as those in Fig. 11. The error bars indicate the variation in the data from five patches in symmetric solutions containing 150 mol/m^3 KCl. The solid curves show the least-squares fit of the diffusion-limited pore model to the data (*see* Discussion). The parameters of this fit are summarized in Table 2. The intrinsic *I/V* characteristics of the channel are linear (*not shown*) so that the voltage saturation seen here arises solely from diffusion-limitation effects

This is based on the finding that at [KCl] > 300 mol/m^3 and [KCl] < 10 mol/m^3, where diffusion-limitation effects are small (*see* previous section), the *I/V* characteristic for the channel in symmetric solutions is nearly linear. The electrodiffusion model can be well approximated by Eqs. (A1)–(A3) when the number of energy barriers in the pore is large (greater than 4, *see* Appendix). In this pore model an arbitrary large number of identical ion sites is chosen (we use here $n = 9$) where the solutions to Eq. (A3) are shown by Läuger (1973).

Third, it is assumed that the "measured" values of P_c are modulated by the ion buffering effects of fixed charges at the mouth of the pore (*see* Jordan, 1987). At high ion concentrations the fixed charges will have little effect on the ion concentration near the pore so that the capture radius of the pore can be estimated from P_c using Eq. (A4). However, at low ionic strength the ion concentration near the pore will be higher than that in the bulk phases. This will increase the effective value of P_c at low ion concentrations. Surface charge need not increase the intrinsic conductance of the pore (Takeda, Gage & Barry, 1982). Further, numerical solutions to the Nernst-Plank-Poisson equations for this pore model (*unpublished data*) indicate that fixed charge at the mouth of the pore can increase P_c without greatly affecting the intrinsic conductance of the pore. The ion buffering effects of fixed charge near the pore mouth is included in the model by letting P_c follow the empirical equation

$$P_c = P_\infty \cdot \{1 + A \cdot \exp([\mathrm{KCl}]/B)\} \quad (4)$$

Table 2. The parameter values of the least-squares fit of the diffusion-limited pore model to the data in Fig. 12[a]

K_m	mol/m^3	50 ± 25
G_{max}	pS	300 ± 20
P_L	10^{-18} m^3/sec	1.1 ± 0.1
A		3.8 ± 1.0
B	mol/m^3	85 ± 10

[a] The errors indicate 90% confidence limits.

where A and B are constants and P_∞ is the value of P_c at high [KCl].

High concentrations of Ca^{2+} (>50 mol/m^3) on the outside of the patch produced a substantial voltage-dependent block of this channel (*unpublished data*) which indicated a K_m for Ca^{2+} binding to the channel given by

$$K_m^{Ca} = 50 \cdot \exp(0.2\, FV_m/RT) \text{ (mol/m}^3\text{)}. \quad (5)$$

In these experiments, though [Ca^{2+}] in the external medium is small, the presence of Ca^{2+} has a small measurable effect on the observed *I/V* characteristics. The predictions of the model allow for competitive binding of Ca^{2+} and K^+ with the channel.

The parameters of the fit are K_m, G_{max} (the maximum conductance), A, B, and P_∞. The values of these parameters are given in Table 2.

The resulting least-squares fit of this model to the data in Fig. 12 indicates that the channel is sig-

nificantly diffusion limited over the concentration range 20–300 mol/m^3. As [KCl] decreases below 20 mol/m^3, the conductance of the pore decreases more rapidly than that of the aqueous convergence regions because of the buffering effect of fixed charge near the pore mouth; thus the pore conductance becomes dominant. As [KCl] increases above 300 mol/m^3, the conductance of the pore now increases more slowly than that of the aqueous convergence regions because the pore saturates; thus here, too, the pore conductance becomes dominant. Calculating the convergence conductance, G_c, using Eq. (A5) with $C_1 = 150$ mol/m^3 and $P'_c = P''_c = 12 \times 10^{-18}$ m^3/sec gives $G_c = 700$ pS, which compares with 270 pS for the expected intrinsic conductance of the pore. In this situation the 60% of the transmembrane potential difference appears across the pore.

The value of P_∞ suggests an ion capture radius for the pore of 0.17 nm, consistent with a pore radius of at least 0.32 nm (using Eq. (A6)), which is about that expected for the maxi-K channel (Latorre & Miller, 1983; Jordan, 1987).

Comparison with Other Maxi-K Channels

The magnitude of possible diffusion-limitation effects in maxi-K channels has been the subject of some concern. The conceptual difficulty lies in the fact that for diffusion-limitation effects to be small enough to allow for the large unitary currents observed in maxi-K channels, the pore should then possess a large capture radius and hence a larger diameter (>1 nm; *see* Jordan, 1987). However, the high ion selectivity of the pore indicates that it should have a much smaller diameter (approximately 0.4 nm). In reconciling this paradox people have either evoked special geometric models (Latorre & Miller, 1983) or, as in this study, postulated the presence of fixed charge distributions about the channel mouth (Jordan, 1987), which obviate the effects of diffusion limitation.

Measurements of K^+ current through maxi-K channels in *Chara australis* (Lühring, 1986; Laver & Walker, 1987; the present study), skeletal and smooth muscle (Eisenman, Latorre & Miller, 1986; Cecchi et al., 1987) and from chromaffin cells (Yellen, 1984) all show characteristics expected from diffusion limitation. We consider here the particular case of the Ca^{2+}-activated K^+ channel from skeletal muscle, inserted in lipid bilayers by Eisenman et al. (1986) because it offers a broad data set for comparison. The concentration- and voltage-dependences of K^+ permeation of the Ca^{2+}-activated K^+ channel (*data not shown*) shows the same form as that for the maxi-K channel in *C. australis*. The analysis of the data from both systems followed a similar path and shared similar difficulties. The outcome of the analysis is that it is possible for diffusion limitation to have a strong effect on the permeation characteristics of the Ca^{2+}-activated K^+ channel. It is also possible to account for the magnitude of the current through the channel with plausible values for the capture radius of the pore ($r_o \approx 0.1$–0.2 nm for [KCl] > 200 mol/m^3).

The saturation of the current at large membrane potentials seems to be an intrinsic property of the channel, unlike that found for the maxi-K channel in *Chara* in which the saturation is derived solely on diffusion-limitation effects. The best fits to the data were obtained for pore models that exhibited two saturating processes with high and low affinities for K^+. This behavior has been observed in maxi-K channels (Moczydlowski et al., 1985) and is believed to be due to either multi-ion occupancy of the pore (Moczydlowski et al., 1985) or to fixed charges in the pore (Barry, Gage & Van Helden, 1979 (*see* Appendix A); Jordan, 1987).

Therefore it is possible that the observed permeation characteristics (e.g. large conductance) of maxi-K channels, in general, are significantly affected by ion diffusion in the aqueous regions adjacent to the pore mouths. As previously suggested by Yellen (1984), investigations similar to those of Andersen (1983) should be made to test for the magnitude of diffusion-limiting effects in different maxi-K channels. Channels inserted into lipid bilayers would be the ideal system in which to study this effect.

Comparison of Ion Permeation in Attached and Excised Patches

At low ion concentrations the currents in attached patches were larger than those in excised patches. This effect remained when the osmotic potentials on each side of the patch were equalized. The drop-attached patches were in contact with cytoplasm on the inside face, which is believed to contain 100 mol/m^3 K^+ (Reeves, Shimmen & Tazawa, 1985), whereas excised patches were usually in symmetric KCl solutions. The *I/V* data obtained from the maxi-K channel in drop-attached and excised patches differ only partly as a result of the different potassium concentrations in each system. The data in Fig. 3 show that at potentials of −100 and −150 mV the composition of the solution on the inside face is not important.

Thus there is a factor, present only in the intact cytoplasmic drop, that enhances the potassium permeation through the channel at low ionic strengths. This is consistent with the presence of negative sur-

face charge either associated with the pore or distributed over the surface of the membrane which is lost during the process of excising the patch. The effects of fixed charges, situated near the pore entrance and on the membrane lipids, on the permeation characteristics of gramicidin and maxi-K channels has been well studied (Apell, Bamberg & Läuger, 1979; Bell & Miller, 1984; Moczydlowski et al., 1985).

The potential-dependence of seal formation and stability, regardless of the presence of maxi-K channels in the patch (*see* Results), further indicates that there is negative surface charge on the membrane, not associated with the channel. Seal breakdown at negative pipette potentials implies electrostatic repulsion between the pipette and the membrane surface charge. The voltage-independent seal stability in excised patches is also consistent with the loss of this charge.

The asymmetry of the I/V data from excised patches in symmetric solutions could arise from differences in the ion capture radius or fixed charge distributions at each end of the pore, or from intrinsic asymmetry in the energy barrier profile for permeable ions within the pore.

Conclusions

The permeation of K^+ ions through the *Chara* maxi-K channel is limited by their diffusion between the bulk phases and the mouths of the pore. Diffusion-limitation effects appear to be significantly moderated, when the ion concentrations are less than 150 mol/m^3, possibly by the presence of fixed charge near the pore mouths.

The diffusion-limited pore model can account for the current saturation at large membrane potentials and for the attenuating action of increasing aqueous viscosity on the pore conductance. The model predicts that the permeation of ions through the channel will be most diffusion-limited for [KCl] in the range 20–300 mol/m^3. The intrinsic permeation properties of the channel are consistent with a pore whose current is limited at high concentrations by the maximum transport rate of the pore.

Maxi-K channels in animal cells have similar permeation characteristics to those of the channel studied here, and it is possible that other maxi-K channels are also diffusion limited. Ion permeation properties of the channel are altered when membrane patches are excised from the cytoplasmic drops. The voltage-dependent stability of the pipette-membrane seal and the attenuation of unitary currents in excised patches can be understood if there exists negative surface charge on the drop membrane which is not present in excised patches. The asymmetry of the I/V characteristics of the maxi-K channel in symmetric KCl solutions indicates an asymmetric chemical structure for the channel.

We wish to thank Drs. Mary Beilby and David Cook for critically reading this manuscript, Dr. Peter Barry for helpful discussions, and the referees for their helpful comments. We acknowledge support from the ARGS and from the University of Sydney. The work was also supported by a National Research Fellowship.

References

Andersen, O.S. 1983. Ion movement through gramicidin A channels: Studies on the diffusion-controlled association step. *Biophys. J.* **41**:147–165

Andersen, O.S., Procopio, J. 1980. Ion movement through gramicidin A channels. On the importance of the aqueous diffusion resistance and ion-water interactions. *Acta Physiol. Scand. Suppl.* **481**:27–35

Apell, H.J., Bamberg, E., Läuger, P. 1979. Effects of surface charge on the conductance of the gramicidin channel. *Biochim. Biophys. Acta* **552**:369–378

Barrett, J.N., Magleby, K.L., Pallotta, B.S. 1982. Properties of single calcium-activated potassium channels in cultured rat muscle. *J. Physiol. (London)* **331**:211–230

Barry, P.H., Diamond, J.M. 1970. Junction potentials, electrode standard potentials, and other problems in interpreting electrical properties of membranes. *J. Membrane Biol.* **3**:93–122

Barry, P.H., Gage, P.W. 1984. Ionic selectivity of channels at the end-plate. *In:* Ion Channels: Molecular and Physiological Aspects. W.D. Stein, editor. Ch 1, pp. 1–51. Academic, New York

Barry, P.H., Gage, P.W., Van Helden, D.F. 1979. Cation permeation at the amphibian motor end-plate. *J. Membrane Biol.* **45**:245–276

Bell, J., Miller, C. 1984. Effects of phospholipid surface charge on ion conduction in the K^+ channel of sarcoplasmic reticulum. *Biophys. J.* **45**:279–287

Blatz, A.L., Magleby, K.L. 1987. Calcium-activated potassium channels. *Trends Neurosci.* **10**:463–467

Cecchi, X., Wolff, D., Alvarez, O., Latorre, R. 1987. Mechanisms of Cs^+ blockade in a Ca^{2+}-activated K^+ channel from smooth muscle. *Biophys. J.* **52**:707–716

Eisenman, G., Latorre, R., Miller, C. 1986. Multi-ion conduction and selectivity in the high-conductance Ca^{++}-activated K^+ channel from skeletal muscle. *Biophys. J.* **50**:1025–1034

Hamill, O.P., Marty, A., Neher, E., Sakmann, B., Sigworth, F.J. 1981. Improved patch-clamp techniques for high-resolution current recording from cells and cell-free membrane patches. *Pfluegers Arch.* **391**:85–100

Harned, H.S., Shropshire, J.A. 1958. The diffusion coefficient at 25° of potassium chloride at low concentrations in 0.25 molar sucrose solutions. *J. Am. Chem. Soc.* **80**:5652–5653

Jordan, P.C. 1987. How pore mouth charge distributions alter the permeability of transmembrane ionic channels. *Biophys. J.* **51**:297–311

Kamiya, N., Kuroda, K. 1957. Cell operation in *Nitella:* I. Cell amputation and effusion of the endoplasm. *Proc. Jpn. Acad.* **33**:149–152

Kundu, K.K., Das, A.K. 1979. Transfer free energies of some ions from water to dimethylsulfoxide-water and urea-water mixtures. *J. Sol. Chem.* **8**:259–263

Latorre, R., Miller, C. 1983. Conduction and selectivity in potassium channels. *J. Membrane Biol.* **71:**11–30

Läuger, P. 1973. Ion transport through pores: A rate-theory analysis. *Biochim. Biophys. Acta* **311:**423–441

Läuger, P. 1976. Diffusion-limited ion flow through pores. *Biochim. Biophys. Acta* **455:**493–509

Laver, D.R., Walker, N.A. 1987. Steady-state voltage-dependent gating and conduction kinetics of single K^+ channels in the membrane of cytoplasmic drops of *Chara australis*. *J. Membrane Biol.* **100:**31–42

Lühring, H. 1986. Recording of single K^+ channels in the membrane of cytoplasmic drop of *Chara australis*. *Protoplasma* **133:**19–27

Marty, A. 1983. Ca^{2+}-dependent K^+ channels with large unitary conductance. *Trends Neurosci.* **6:**262–265

Moczydlowski, E., Alvarez, O., Vergara, C., Latorre, R. 1985. Effect of phospholipid surface charge on the conductance and gating of a Ca^{2+}-activated channel in planar lipid bilayers. *J. Membrane Biol.* **83:**273–282

Quartararo, N., Barry, P.H. 1987. A simple technique for transferring excised patches of membrane to different solutions for single-channel measurements. *Pfluegers Arch.* **410:**677–678

Reeves, M., Shimmen, T., Tazawa, M. 1985. Ionic activity gradients across the surface membrane of cytoplasmic drops from *Chara australis*. *Plant Cell Physiol.* **26:**1185–1193

Robinson, R.A., Stokes, R.H., Marsh, K.N. 1970. Activity coefficients in the ternary system: Water + sucrose + sodium chloride. *J. Chem. Thermodynam.* **2:**745–750

Sakano, K., Tazawa, M. 1986. Tonoplast origin of the membrane of cytoplasmic droplets prepared from *Chara* internodal cells. *Protoplasma* **131:**247–249

Takeda, K., Gage, P.W., Barry, P.H. 1982. Effects of divalent cations on toad end-plate channels. *J. Membrane Biol.* **64:**55–66

Yellen, G. 1984. Ionic permeation and blockade in Ca^{2+}-activated K^+ channels of bovine chromaffin cells. *J. Gen. Physiol.* **84:**157–186

Zimmerberg, J., Parsegian, V.A. 1986. Polymer inaccessible volume changes during opening and closing of a voltage-dependent ionic channel. *Nature (London)* **323:**36–39

Received 19 August 1988; revised 22 November 1988

Appendix

The theory of diffusion-limited ion flow through pores has been developed by Läuger (1976). He considered a simple geometrical model of a pore, consisting of a right circular cylinder separating two aqueous phases (denoted by ′ and ″). The current was assumed to converge and diverge with spherical symmetry at the pore entrances. The net passive ion flux, J, through such a system in which there is a permeant cation species, a nonpermeant cation species, and one nonpermeant anion species was shown to be given by the following set of three simultaneous equations:

$$J = -2P_c'C_2' \cdot (y' - 1) \tag{A1}$$

$$J = 2P_c''C_2'' \cdot (y'' - 1) \tag{A2}$$

$$J = k_o' K \frac{C_p' - UC_p''}{\sum_1^n \bar{R}_i \left(1 + \sum_1^n S_i\right) + KC_p'Q' + KUC_p''Q''} \tag{A3}$$

where P_c' and P_c'' are the permeation constants[4] (in units of m^3/sec) for the aqueous convergence regions. $y' \equiv \exp(\Phi_p' - \Phi')$ and $y'' \equiv \exp(\Phi_p'' - \Phi'')$ represent the Boltzman factor for the partitioning of monovalent anions between the bulk phases and the mouths of the pore. Φ and Φ_p (in units of F/RT) are the dimensionless electric potentials in the bulk phases and the mouths of the pore, respectively. $C_p' \equiv C_2' \cdot y' - C_3'/y'$ and $C_p'' \equiv C_2'' \cdot y'' - C_3''/y''$ are the concentrations of the permeant cations at the pore mouths. C_1 (not explicit in Eqs. (A1)–(A3)), C_2 and C_3 are the concentrations of the permeant cation, anion and nonpermeant cation species, respectively. $U \equiv \exp(V) \cdot y'/y''$ is the exponential of the potential difference across the pore. V is the potential difference between the two bulk phases ($V = \Phi' - \Phi''$). K is the equilibrium constant for binding between K^+ and the pore.

Equations (A1) and (A2) (Läuger, 1976) give the ion flux in terms of the properties of the convergence regions. Equation (A3) is derived using the rate theory approach by Läuger (1973). Equation (A3) describes the ion flux through a pore with n sequential energy minima (binding sites) which holds, at most, one ion. This equation has the form of the Michaelis-Menten equation where the voltage-dependent terms, $\bar{R}_i$, S_i, Q, and k_o' depend on the energy profile of the channel. When n is large the predictions of the rate theory and the electrodiffusion model are the same. However, even for as few as three ion sites the rate theory predictions approach those of the continuum electrodiffusion model (Barry & Gage, 1984).

P_c can be expressed in terms of the diffusion constant D of the permeant ion species, the aqueous phases and the capture radius r_o for the channel entrance (Läuger, 1976).

$$P_c = 2\pi r_o D. \tag{A4}$$

In symmetrical ionic conditions the conductance of the convergence regions G_c, like that of the pore, is related to the permeation constants by

$$G_c = (F^2/RT)C_1P_c. \tag{A5}$$

The capture radius of the channel can be as small as the difference between the ion and pore radii, so the minimum pore radius r_p is related to the ionic radius r_i and the capture radius by

$$r_p = r_i + r_o. \tag{A6}$$

[4] The quantities P_c' and P_c'' represent an area-specific permeance and will be referred to as permeation constants in this paper. Thus P_c' and P_c'' are related to permeability (dimensions of m/sec) · area, hence the dimensions m^3/sec.